Journal of Power Sources Advances 33 (2025) 100176

Contents lists available at ScienceDirect

Journal of Power Sources Advances

journal homepage: www.sciencedirect.com/journal/journal-of-power-sources-advances

Photopolymerized gel polymer electrolytes with cyclic carbonate side chains for Li-organic batteries at room temperature

Öykü Simsek [a,b,c], Philip Zimmer [a,b,c], Simon Muench [a,b], Ulrich S. Schubert [a,b,c,d,*]

[a] Laboratory of Organic and Macromolecular Chemistry (IOMC), Friedrich Schiller University Jena, Humboldtstraße 10, 07743, Jena, Germany
[b] Center for Energy and Environmental Chemistry Jena (CEEC Jena), Friedrich Schiller University Jena, Philosophenweg 7a, 07743, Jena, Germany
[c] Helmholtz Institute for Polymers in Energy Applications Jena (HIPOLE Jena), Lessingstraße 12-14, 07743, Jena, Germany
[d] Helmholtz-Zentrum Berlin für Materialien und Energie, 14109, Berlin, Germany

A B S T R A C T

In this study, we developed gel polymer electrolytes (GPEs) containing cyclic carbonate side chains produced *via* UV-induced free radical polymerization, a fast and cost-efficient synthesis route, for Li-organic batteries. Cyclic carbonate methacrylate (CCMA) was copolymerized with diethylene glycol methyl ether methacrylate (DEGMEM) for 1 h. Then the resultant polymer films were swelled in 1 M $LiPF_6$ in EC/DMC (50/50, v/v) with an electrolyte uptake of 500 %. These novel GPEs with an ionic conductivity of 1.1 mS cm^{-1} at 20 °C were electrochemically tested in Li//PTMA cells in comparison with LP30. They were found to show maximum discharge capacities (62.6 *vs.* 63.9 mAh g^{-1}, GPE *vs.* LP30) at 0.1 C in addition to better compatibility with Li anodes (25.7 *vs.* 40.2 mV overpotential in Li stripping/plating tests) and a comparable electrochemical stability window. The results confirm that these GPEs are promising candidates for Li-organic batteries.

1. Introduction

Organic radical batteries (ORB) have attracted great attention in the last years since they provide reversible and fast redox kinetics with more environmentally friendly materials, which can be obtained from abundant resources cheaply, designed with different electronic properties, and recycled easily. Organic electrode materials can be categorized into n-type and p-type based on the type of charge in the charged state. N-type materials take up cations and show lower potentials than p-type materials and usually display higher specific capacities [1]. Contrarily, p-type ones interact with anions and show comparatively higher potential (>3.5 V *vs.* Li/Li^+), and therefore can be used as cathode materials [1,2]. Among them, poly(2,2,6,6-tetramethyl-1-piperidinyloxy methacrylate) (PTMA) is the most comprehensively researched organic cathode material since it was first reported by Nakahara et al. in 2002 [3]. It features a specific capacity of 111 mAh g^{-1} in conjunction with high rate capability and good cycling stability when combined with state-of-art lithium ion battery (LIB) electrolytes like 1.0 M lithium hexafluorophosphate ($LiPF_6$) in ethylene carbonate (EC)/dimethyl carbonate (DMC) (LP30) or 1.0 M $LiPF_6$ in EC/diethyl carbonate (DEC) [4–6].

Despite providing good cell performance with organic cathodes and revealing high ionic conductivity, the leak risk of flammable and volatile conventional LIB electrolytes causes safety concerns including fire and explosion. Solid polymer electrolytes (SPEs), polymer matrices containing metal salts, are considered as safer systems, although they suffer from low ionic conductivities between 10^{-6} and 10^{-4} S cm^{-1} [7]. Gel polymer electrolytes (GPEs), where a liquid electrolyte (LE) is immobilized in a polymer matrix, show higher ionic conductivities than SPEs, in addition to both superior mechanical strength and flexibility. Consequently, they can substitute conventional separators and overcome the possible safety issues.

According to literature, GPEs are rarely preferred for Li//PTMA batteries. Fibrous poly(vinylidene fluoride-*co*-hexafluoropropylene) (PVdF-HFP) membranes were immersed in 1 M $LiPF_6$ in EC:DMC (1:1, vol:vol) by Kim et al. [8] The GPEs were found to have 240 % of electrolyte uptake and 7.3 x 10^{-3} S cm^{-1} of ionic conductivity at 25 °C. 111 mAh g^{-1} of specific capacity was obtained in Li//PTMA cells having 17 μm thick PTMA electrodes. Only 68 mAh g^{-1} was obtained for the same type of cell with 36 μm thick PTMA electrodes. In another work, GPEs were manufactured *via* soaking the same membranes in 1 M lithium bis(trifluoromethanesulfonyl)imide (LiTFSI) in 1-butyl-1-methylpyrrolidinium bis(trifluoromethylsulfonyl)imide ($Pyr_{14}TFSI$). Specific capacities of 110 mAh g^{-1} at 1C and 80 mAh g^{-1} at 10C were observed [9].

In this work, GPEs with cyclic carbonate groups are fabricated *via* UV-induced polymerization. Previously, GPEs based on cyclic carbonate

* Corresponding author. Laboratory of Organic and Macromolecular Chemistry (IOMC), Friedrich Schiller University Jena, Humboldtstraße 10, 07743, Jena, Germany.
E-mail addresses: ulrich.schubert@uni-jena.de, publications.agschubert@uni-jena.de (U.S. Schubert).

https://doi.org/10.1016/j.powera.2025.100176
Received 15 January 2025; Received in revised form 13 March 2025; Accepted 30 March 2025
Available online 23 April 2025

methacrylate (CCMA) and oligo(ethylene glycol) methyl ether methacrylate (OEGMA) were developed by Lex-Balducci et al. [10] In their next study [11], the authors demonstrated that ethylene oxide (EO) groups are involved in the interaction with Li^+ ions reducing their mobility and overall conductivity of the GPE. Therefore, in this work, CCMA is combined with diethylene glycol methyl ether methacrylate (DEGMEM) having a shorter EO chain. In contrast to the previous work of Lex-Balducci et al., GPEs are tested in Li//PTMA cells instead of graphite//lithium nickel manganese cobalt oxide (NMC) full cells. For the preparation of GPEs, CCMA was copolymerized with DEGMEM under UV-irradiation under ambient conditions in presence of benzophenone, a literature-known UV-initiator that induces crosslinking of the polymer chains as well, for 1 h [12,13]. The received films were punched out, dried, and immersed in 1 M $LiPF_6$ in EC:DMC (1:1, vol:vol) (LP30). The electrochemical characteristics were investigated in comparison with pristine LP30, where the GPEs revealed similar capacities at 0.1C and 5C with better cycling stability at long-term cycling.

2. Experimental

Diethylene glycol methyl ether methacrylate (DEGMEM) and glycerol carbonate methacrylate (CCMA) were purchased from TCI and abcr, respectively. Benzophenone and carbon black (Super P) were bought from Alfa Aesar. 1.0 M $LiPF_6$ in EC/DMC (LP30) and carboxymethyl cellulose (CMC) were received from Sigma-Aldrich. The inhibitors in CCMA and DEGMEM were removed *via* an inhibitor remover from Sigma-Aldrich. Carbon black (Super P) was purchased from Alfa Aesar.

2.1. Fabrication of cathodes

PTMA was synthesized by polymerization of 2,2,6,6-tetramethyl-4-piperidyl methacrylate and triethyleneglycol dimethacrylate (4 mol%) as crosslinker using 4,4′-azobis(4-cyanovaleric acid) (5 mol%) as initiator in MeOH/H_2O (1.5 mol L^{-1} monomer concentration) at 70 °C for 24 h. The resulting precursor polymer was ball milled and oxidized using 3 eq. of H_2O_2 catalyzed by $MgSO_4$ (2 mol%) in water to yield PTMA particles.

The electrodes were prepared by mixing 60 wt% PTMA, 35 wt% SuperP, and 5 wt% CMC, with water in a lab dissolver (Dispermat®, VMA-GETZMANN) to form a homogeneous viscous paste. Subsequently, this slurry was doctor-bladed on aluminum foil and dried at 80 °C overnight. The resulting composite electrodes were punched at a diameter of 12 mm with active material loadings of *ca.* 1.4 mg cm^{-2}. The discs were vacuum dried at 80 °C for 12 h prior to use.

2.2. Fabrication of GPE

For the fabrication of GPEs (Scheme 1), CCMA and DEGMEM were mixed in the weight ratio of 1–3, benzophenone was added (2 wt%). The mixture was placed between two Mylar foils and UV-irradiated for 1 h using a UV cube (mercury lamp, 0.175 W cm^{-2}, Dr. Hönle AG). The obtained free-standing polymer films were punched out and vacuum-dried at 120 °C for 24 h. The polymer discs were soaked in LP30 (weight ratio polymer:electrolyte 1:5) (Fig. S1) in a glovebox (H_2O < 2 ppm, O_2 < 2 ppm).

2.3. Materials characterization

The kinetics analysis of GPEs was performed *via* ^{1}H NMR spectroscopy. For this purpose, the GPE precursor was freshly prepared and dimethyl formamide (DMF) was added as internal standard. Subsequently, this solution was analyzed with ^{1}H NMR spectroscopy. After applying UV-irradiation to the precursor for 15 min, 30 min, 45 min, and 60 min, the resulting samples were stirred in DMSO-d6 overnight. Thereafter, the mixtures were filtered, and the obtained solutions were analyzed using ^{1}H NMR measurements. ^{1}H NMR results of the GPE precursor before UV-polymerization: (300 MHz, $CDCl_3$, δ in ppm): 6.12–6.19 (CCMA, DEGMEM, MA sp^2); 5.56–5.69 (CCMA, DEGMEM, MA sp^2); 4.98 (CCMA, sp^3); 4.59 (CCMA, sp^3); 4.28–4.48 (CCMA, DEGMEM, sp^3); 3.52–3.79 (DEGMEM, sp^3); 3.40 (DEGMEM, sp^3); 1.94–1.98 (CCMA, DEGMEM, MA sp^3).

Before the thermogravimetric analysis (TGA), the non-swollen polymer disc was vacuum-dried at 120 °C overnight. The measurements were performed using a temperature range of 25–600 °C with a heating rate of 10 K min^{-1} (Netzsch TG 209F1, under nitrogen).

For temperature-dependent conductivity measurements, the GPEs were placed in a closed cell (TSC Battery cell, rhd instruments) between two stainless steel (SS) electrodes and measured at temperatures from 0 to 50 °C in a climatic chamber (Binder-Alternating Climate Chamber MK056). Electrochemical impedance spectroscopy (EIS) was carried out within the frequency range of 1 MHz–10 Hz with the amplitude of 20 mV. The bulk resistance R_{bulk} of the electrolyte was determined by fitting the Nyquist spectra linearly, with a series of inductors, resistance, and constant phase element. RelaxIS 3 Impedance Spectrum Analysis Version 3.0.23 Build 24 was used for modeling the impedance spectra. The modeled resistance is assumed as bulk resistance and used for conductivity calculation with the equation

$$\sigma = \frac{t}{A\,R_{bulk}}$$

where t represents the distance the current travels through the sample, equal to the thickness of the samples, and A the contact area of the sample to the electrodes, which is assumed constant with radius of 4 mm.

Stripping-plating tests of Li/LP30/Li and Li/GPE/Li coin cells built in an Ar-filled glovebox were executed for ten cycles at current densities of 0.01, 0.02, 0.05, and 0.1 mA cm^{-2}, 2 h each with a limited potential between −2 and 2 V, and long-term cycling at 0.02 mA cm^{-2} at a Bio-Logic VSP and VMP-300 potentiostat/galvanostat.

Li/LP30/SS and Li/GPE/SS Swagelok cells were assembled in the

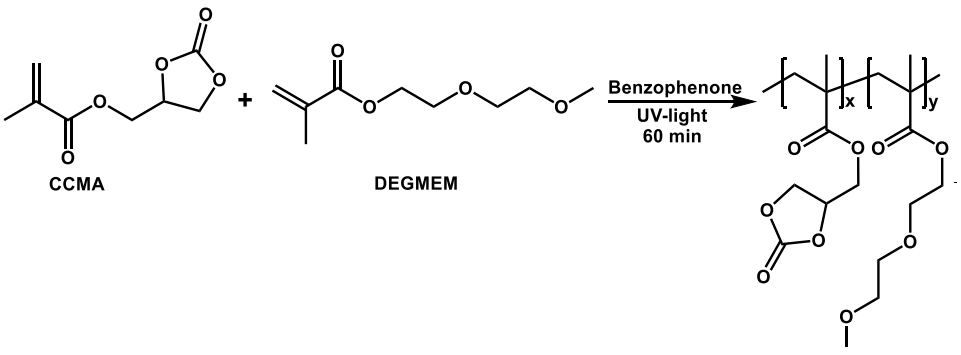

Scheme 1. Schematic representation of the synthesis of GPEs.

glovebox and used for linear sweep voltammetry (LSV) measurements conducted between −0.5 and 5.5 V with a scanning rate of 1 mV s^{-1} at a BioLogic VSP potentiostat/galvanostat.

Li/LP30/PTMA and Li/GPE/PTMA coin cells were built in glovebox and operated for three cycles at 0.1C, five cycles at 0.2C/0.5C/1C/2C/5C each and long-term cycling at 1C between 3 and 4 V at a BioLogic BCS-900 battery cycler.

3. Results and discussion

3.1. ^1H NMR kinetic studies

^1H NMR kinetic studies were carried out and the conversion of monomers during photopolymerization was calculated (Fig. S2). Over 85 % of conversion is achieved after 15 min and over 99 % after 30 min. Even if the monomer conversion is complete, the film formation still proceeds due to the continuing crosslinking mechanism. The excited benzophenone abstracts the hydrogen atoms from the side chains resulting in recombination of the macroradicals [13]. Therefore, 60 min was chosen as polymerization time.

3.2. Thermogravimetric analysis

The thermal behaviors of LP30, the GPE, and the pristine polymer (polymer film before swelling) were evaluated *via* thermogravimetric analysis (TGA) (Fig. S3). The decomposition temperature (T_d) is specified as the temperature of 5 % mass loss. The pristine polymer displays a T_d of 244 °C, while it is 83 °C for LP30 since it comprises quite volatile DMC. However, the GPE starts to decompose at 126 °C, which reveals that the interaction between the polymer and LP30 impedes the evaporation of LP30 [10] and increases the safety of the electrolyte. The results show that both electrolytes are suitable for the operation at room temperature.

3.3. Electrochemical stability window

Linear sweep voltammetry (LSV) was applied to the Li/LP30/SS and Li/GPE/SS Swagelok cells and the found electrochemical stability windows (ESW) are plotted in Fig. 1.

The electrolytes all behave in the same manner and the oxidative and reductive decompositions start at over 5 V and below 0 V *vs.* Li, respectively, for both samples. Processes observed below 1.5 V can be assigned to the reduction of EC [14,15]. Other peaks close to 1.5 and 1.8 V revealed by LP30 and at 1.8 V by GPE are similar to the values reported for the formation of SEIs [16]. The sudden decrease below 0 V corresponds to the metallic lithium plating [17]. Considering the galvanostatic cycling tests operated between 3 and 4 V due to the active material of PTMA showing a redox potential of 3.6 V *vs.* Li/Li^+, it can be concluded that the GPE maintains the sufficient electrochemical stability of LP30.

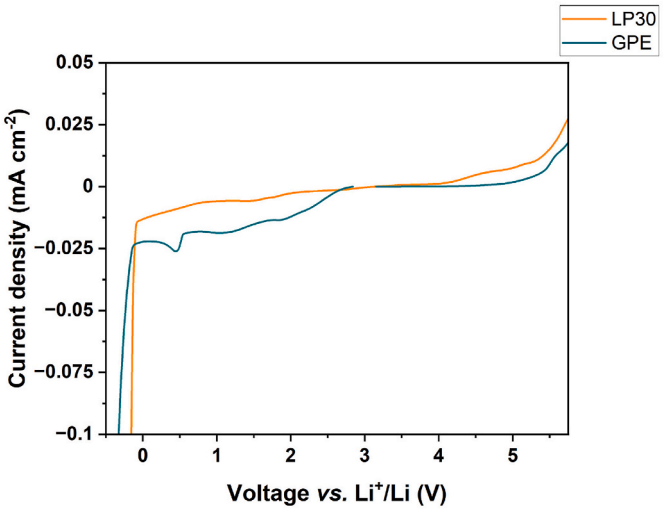

Fig. 1. Electrochemical stability window of LP30 and GPE.

3.4. Electrochemical impedance spectroscopy

The impedance values at different temperatures between 0 and 50 °C of three GPE samples were measured. In most cases, straight lines are obtained. Nevertheless, for one of the samples, a semi-circle with a significantly higher impedance at 0 °C is present (Fig. S4). In view of the freezing point of EC at 36 °C, a capacitance derived from a frozen layer could be the reason for this observation. For this reason, this value is not involved in the analysis. For the remaining data, the calculated ionic conductivities are plotted in comparison with the reported values of LP30 in literature [18] (Fig. 2).

Expectedly, LP30 demonstrates much higher ionic conductivities starting from 6.1 mS cm^{-1} at 0 °C reaching 18.1 mS cm^{-1} at 50 °C. Although the GPE presents lower ionic conductivities of 0.4 mS cm^{-1} at 0 °C and 2.6 mS cm^{-1} at 50 °C, the obtained values are good considering the other studies about GPEs containing LP30 in literature [14,19]. Furthermore, the ionic conductivity benchmark of 1 mS cm^{-1} making the system suitable for practical applications [20] is already achieved at 20 °C with 1.1 mS cm^{-1}. Based on these results, the GPE has sufficient ionic conductivity for potential applications.

3.5. Lithium stripping-plating tests

The electrochemical stability of the electrolytes was evaluated by stripping-plating tests carried out at 0.01, 0.02, 0.05, 0.1 mA, and 0.02 mA cm^{-2} as plotted in Fig. 3. At the first step, both electrolytes reveal smoothly shaped profiles with an initial overpotential of 15.4 mV slightly increasing to 16.1 mV for LP30 and a decreasing trend from 28.8 mV to 13.5 mV for the GPE. This trend can be attributed to the restructuring of the interface between the lithium metal and the electrolyte and evolving to the solid electrolyte interphase (SEI) [21]. While the GPE keeps its smooth cycles with a minor rise in overpotential resulting in 14 mV, it becomes 18 mV with a sharper shape for LP30 at 0.02 mA cm^{-2}. As the current density increases, the difference between the overpotentials also increases. Consequently, 25.7 mV with a still

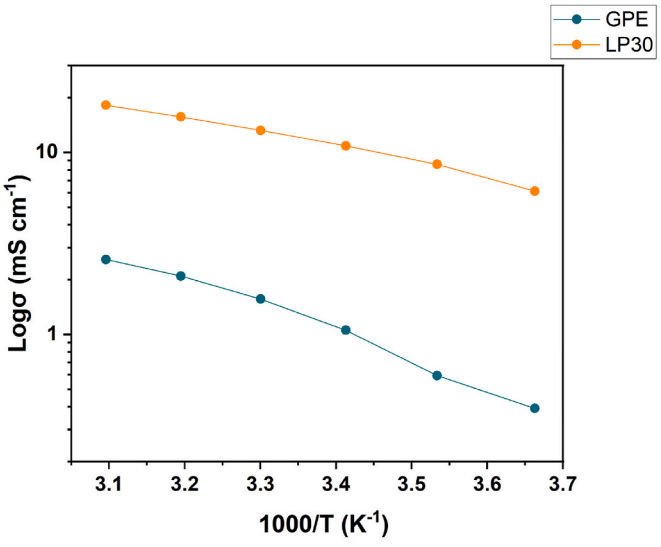

Fig. 2. Temperature-dependent ionic conductivity of LP30 [18] and the studied GPE.

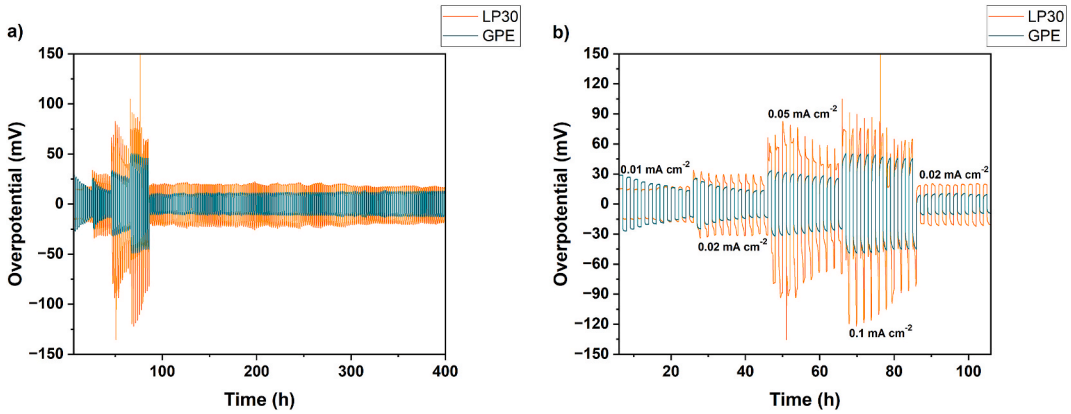

Fig. 3. Voltage/time profiles of LP30 and GPE: a) During 400 h and b) zoom at different current densities.

stable cycling behavior for the GPE and, in case of LP30, 40.2 mV with unsymmetrical curves evolving from peaking to arcing behavior attributed to the accumulation of dead Li on the Li surface, are present at 0.05 mA cm^{-2}. The higher current density of 0.1 mA cm^{-2} leads to even more unstable overpotentials with spikes, which can arise from the dendrite formation and thermo-fusible effect [22] for LP30 within the same cycling regime. Nevertheless, the GPE maintains its arcing behavior in conjunction with a slight increase to 45.5 mV. At the last step, the initial overpotential of 19 mV belonging to LP30 decreases to 17 mV at the end of 400 cycles in total. The GPE, however, starts with an overpotential of 9 mV, which is less than half of the value of LP30, and finishes with only 13 mV. In general, the GPE demonstrates lower overpotentials with more stable cycling behavior compared to LP30 due to its possibly higher compatibility with Li metal and better dendrite inhibition behavior.

3.6. Galvanostatic cycling tests

For the galvanostatic cycling tests, Li/LP30/PTMA and Li/GPE/PTMA coin cells were assembled and evaluated in terms of rate capability and long-cycling tests (Fig. 4). The maximum specific discharge capacity of cells with LP30 of 63.6 mAh g^{-1} is shown at 0.1C. Cells with the GPE deliver nearly the same value of 62.9 mAh g^{-1} at the same C-rate. At 0.5C, the GPE exhibits up to 48.8 mAh g^{-1}, which is close to the 53.7 mAh $g^{-1}$of LP30. An increasing C-rate results in an increase in the difference between the capacities, which amount to 45.7 mAh g^{-1} in case of LP30 and to 40.3 mAh g^{-1} for GPE at the first-applied 1C. Contrarily, at 5C, rather similar capacities are observed for both systems; 22.8 mAh g^{-1} and 20.8 mAh g^{-1} for LP30 and GPE, respectively.

The long-term stability of the electrolytes was assessed for over 970 cycles at 1C after the rate capability test. Since the performance of GPEs is more susceptible to temperature variations compared to LEs, temperature changes during day and night lead to fluctuating cycling behavior, unlike for LP30. Notwithstanding lower initial discharge capacities (40.9 *vs.* 45.3 mAh g^{-1}), the GPE attains a capacity retention greater than 67 % whilst it is only 54 % for LP30 after 1000 cycles.

The capacities reached by the GPE were found to be comparable to LP30, in particular at 0.1C and 5C. Additionally, the GPE-based cells display a much higher capacity retention after 1000 consecutive cycles in total compared to LP30, whilst eliminating the necessity of a separator and the leakage risk. Given these circumstances, it can be concluded that the GPE offers a cell performance comparable to that of LP30 with an enhanced safety.

4. Conclusion

In summary, gel polymer electrolytes (GPEs) containing cyclic carbonate groups were developed *via* UV-polymerization and swelling in 1.0 M lithium hexafluorophosphate ($LiPF_6$) in ethylene carbonate (EC)/dimethyl carbonate (DMC) (LP30). For the synthesis of the polymer matrix, cyclic carbonate methacrylate was photopolymerized with diethylene glycol methyl ether methacrylate for 1 h with a monomer conversion close to 100 %. The obtained film was punched, and the discs were immersed in LP30 in the glovebox leading to 500 % electrolyte uptake. The GPEs display good ionic conductivities of 1.1 mS cm^{-1} at 20 °C and 2.6 mS cm^{-1} at 50 °C coupled with similar anodic stability (over 5 V), as well as lower and stable overpotentials (25.7 *vs.* 40.2 mV at 0.05 mA cm^{-2}). The electrochemical performances of the electrolytes were investigated in Li//poly(2,2,6,6-tetramethyl-1-piperidinyloxy methacrylate) (PTMA) cells and similar capacities were found (63.6 *vs.* 62.9

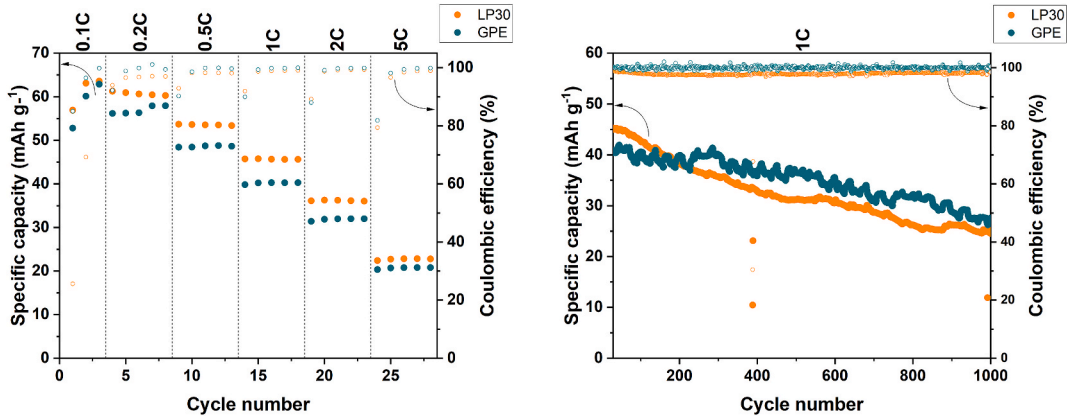

Fig. 4. Galvanostatic charge-discharge tests of LP30 and GPE: a) During rate capability and b) long cycling.

mAh g^{-1} at 0.1C for LP30 and GPE, respectively). Considering these results, the developed GPE represents a promising candidate for Li-organic batteries.

CRediT authorship contribution statement

Öykü Simsek: Conceptualization, Methodology, Investigation, Validation, Data curation, Formal analysis, Visualization, Writing – original draft. **Philip Zimmer:** Formal analysis (supporting), Writing – original draft. Simon Muench: Supervision (of Ö. S.), Writing – review & editing. **Ulrich S. Schubert:** Writing – review & editing, Supervision (of Ö.S. and P.Z.), Funding acquisition.

Declaration of competing interest

The authors declare the following financial interests/personal relationships which may be considered as potential competing interests: Ulrich S. Schubert reports financial support was provided by European Union. If there are other authors, they declare that they have no known competing financial interests or personal relationships that could have appeared to influence the work reported in this paper.

Acknowledgement

The authors would like to acknowledge the financial support from the European Union's Horizon 2020 research and innovation program under the Marie Skłodowska-Curie grant agreement No 860403 "POLYSTORAGE".

Appendix A. Supplementary data

Supplementary data to this article can be found online at https://doi.org/10.1016/j.powera.2025.100176.

Data availability

Data will be made available on request.

References

[1] A. Innocenti, I.Á. Moisés, O. Lužanin, J. Bitenc, J.-F. Gohy, S. Passerini, ACS Appl. Mater. Interfaces 16 (2023) 48757–48770.
[2] H. Kye, Y. Kang, D. Jang, J.E. Kwon, B.-G. Kim, Adv. Energy Sustainability Res. 3 (2022) 2200030.
[3] K. Nakahara, S. Iwasa, M. Satoh, Y. Morioka, J. Iriyama, M. Suguro, E. Hasegawa, Chem. Phys. Lett. 359 (2002) 351–354.
[4] J.-K. Kim, J.-H. Ahn, G. Cheruvally, G.S. Chauhan, J.-W. Choi, D.-S. Kim, H.-J. Ahn, S.H. Lee, C.E. Song, Met. Mater. Int. 15 (2009) 77–82.
[5] K. Nakahara, J. Iriyama, S. Iwasa, M. Suguro, M. Satoh, E.J. Cairns, J. Power Sources 165 (2007) 870–873.
[6] K. Nakahara, J. Iriyama, S. Iwasa, M. Suguro, M. Satoh, E.J. Cairns, J. Power Sources 165 (2007) 398–402.
[7] P. Isken, M. Winter, S. Passerini, A. Lex-Balducci, J. Power Sources 225 (2013) 157–162.
[8] J.-K. Kim, G. Cheruvally, J.-W. Choi, J.-H. Ahn, D.S. Choi, C.E. Song, J. Electrochem. Soc. 154 (2007) A839.
[9] J.-K. Kim, A. Matic, J.-H. Ahn, P. Jacobsson, RSC Adv. 2 (2012) 9795–9797.
[10] S. Tillmann, P. Isken, A. Lex-Balducci, J. Power Sources 271 (2014) 239–244.
[11] S.D. Tillmann, P. Isken, A. Lex-Balducci, J. Phys. Chem. C 119 (2015) 14873–14878.
[12] M. Doytcheva, R. Stamenova, V. Zvetkov, C.B. Tsvetanov, Polymer 39 (1998) 6715–6721.
[13] B. Rupp, M. Schmuck, A. Balducci, M. Winter, W. Kern, Eur. Polym. J. 44 (2008) 2986–2990.
[14] M. Drews, T. Trötschler, M. Bauer, A. Guntupalli, W. Beichel, H. Gentischer, R. Mülhaupt, B. Kerscher, D. Biro, ACS Appl. Polym. Mater. 4 (2021) 158–168.
[15] R. Lundström, N. Gogoi, X. Hou, E.J. Berg, J. Electrochem. Soc. 170 (2023) 040516.
[16] T. Kawaguchi, K. Shimada, T. Ichitsubo, S. Yagi, E. Matsubara, J. Power Sources 271 (2014) 431–436.
[17] X. Dong, Z. Chen, X. Gao, A. Mayer, H.-P. Liang, S. Passerini, D. Bresser, J. Energy Chem. 80 (2023) 174–181.
[18] M. Orbay, D. Leistenschneider, C. Leibing, A. Balducci, Chemelectrochem 10 (2023) e202300171.
[19] S. Davino, D. Callegari, D. Pasini, M. Thomas, I. Nicotera, S. Bonizzoni, P. Mustarelli, E. Quartarone, ACS Appl. Mater. Interfaces 14 (2022) 51941–51953.
[20] G.A. Elia, U. Ulissi, S. Jeong, S. Passerini, J. Hassoun, Energy Environ. Sci. 9 (2016) 3210–3220.
[21] Z. Chen, G.T. Kim, J.K. Kim, M. Zarrabeitia, M. Kuenzel, H.P. Liang, D. Geiger, U. Kaiser, S. Passerini, Adv. Energy Mater. 11 (2021) 2101339.
[22] D. Iermakova, R. Dugas, M. Palacín, A. Ponrouch, J. Electrochem. Soc. 162 (2015) A7060.